



A study on double-cantilever miniaturized FBG acceleration sensors for low-frequency vibration monitoring

Li Hong^{1,2} · Xi Wu^{1,2} · Qiang Gao^{1,2} · Chunming Pei^{1,2} · Kuaikuai Liu^{1,2}

Received: 23 April 2023 / Accepted: 28 June 2023 / Published online: 14 July 2023
© The Author(s), under exclusive licence to The Optical Society of India 2023

Abstract The measurement of low-frequency vibration signals is of great significance for the studies on the seismic monitoring of railway transportation, bridges, and civil building structures. Aiming at the problem that the existing cantilever-type FBG acceleration sensors are difficult to effectively pickup low-frequency vibration signals and that they are large in size, a double cantilever beam-based miniaturized low-frequency FBG acceleration sensor is proposed. Firstly, the vibration model of the acceleration sensor is built, and its working principle is analyzed; secondly, the effect of structural parameters of the sensor on its sensitivity and natural frequency is analyzed, and the structural parameters of the sensor are optimized by the ANSYS simulation software; finally, the real sensor is developed, and a low-frequency vibration test system is set up to test the performance of the sensor. The experiment result suggests that the natural frequency of the sensor is about 71.4 Hz; the low-frequency vibration signals can be effectively picked up in the frequency range of 0.1–2 Hz; favorable linearity is observed in the operating frequency band of 2–50 Hz; the sensitivity is about 1022.8 pm/g, and the dynamic range is 74.5 dB; the transverse interference is not higher than 4.2%, and the volume is merely 7 cm³, which is significantly reduced compared to similar FBG acceleration sensors. The research findings provide a reference for the development of miniaturized low-frequency FBG accelerator sensors.

Keywords Acceleration sensor · Fiber Bragg grating (FBG) · Double cantilever beams · Low-frequency vibration

Introduction

Natural disasters such as earthquakes, tsunamis and landslides may cause the load of large engineering structures such as railway facilities, bridges, dams and civil buildings to change, resulting in safety accidents such as collapses and settlements, which in turn threaten the safety of people's lives and property [1, 2]. Low-frequency vibration measurement techniques can monitor the vibration frequency and vibration mode of structures in real time to ensure their health and timely release the early warning of structural damage [3]. As new sensing elements, FBG acceleration sensors can detect low-frequency vibration signals, and compared with traditional electrical vibration sensors, they provide better solutions in distributed monitoring, corrosion resistance, immunity to electromagnetic interference, multi-point simultaneous measurement, etc., which makes them extensively concerned by researchers [4, 5].

In recent years, many researchers have made great efforts on FBG acceleration sensors [6, 7]. Among them, FBG acceleration sensors based on cantilever beams have been extensively studied due to their simple design, ease of manufacture and high accuracy. Various types of cantilever beam FBG acceleration sensors have emerged in endlessly [8, 9]. Liu et al. [10] proposed an FBG acceleration sensor based on double cantilever beams with small strain gradients, in which the weight of the mass block is 35 g, the volume being about 56 cm³, the flat frequency range being 4–30 Hz, and the sensitivity being limited to 8.58 pm/g. Kok-Sing Lim et al. [11] designed a horizontal cantilever-type FBG acceleration

✉ Qiang Gao
gxtg_cidp_gq@163.com

¹ Institute of Disaster Prevention, Sanhe 065201, Hebei, China

² Hebei Key Laboratory of Seismic Disaster Instrument and Monitoring Technology, Sanhe 065201, Hebei, China

sensor with magnetic damper. The sensor employs magnet as mass block, which works with U-grooves to form a magnetic damper; the overall structure volume is about 70 cm^3 , and the sensitivity is 7.1 pm/g ; it offers excellent linear response in the frequency range of 20–100 Hz. Khan et al. [12] proposed an FBG acceleration sensor based on L-shaped non-uniform section cantilever beams, which enabled the sensor temperature self-compensation by using two FBGs. At resonant frequencies above 150 Hz, the sensor sensitivity is 306 pm/g , but in the frequency range below 50 Hz, the sensor sensitivity is only 46 pm/g . The mass block of the sensor weighs 23 g and its volume is approximately 25 cm^3 . Parida et al. [13] proposed a T-shaped acceleration sensor based on cantilever beam; its natural frequency is as low as 64 Hz, and its sensitivity is 821 pm/g over the operating range of 5–40 Hz. The mass block of the sensor weighs 16 g and its volume is approximately 2 cm^3 . Jiang et al. [14] proposed an FBG acceleration sensor based on a cantilever beam, with two fiber supports installed at both ends of the cantilever beam. The FBG can achieve longitudinal stretching through free end displacement and rotation. The natural frequency of the sensor is 76 Hz, and the sensitivity is 59.3 pm/g . The mass of the mass block is 41 g, and the volume is about 52 cm^3 . Xiang et al. [15] proposed a cantilever fiber Bragg grating accelerometer with a natural frequency of 125 Hz, a sensitivity of 75 pm/g , a mass of 63 g, and a volume of approximately 235 cm^3 . Liu et al. [16] proposed a structure based on double diaphragm. By optimizing the quality factor and increasing the working range, the anti-lateral interference ability is less than 3.6%, the natural frequency is 441.0 Hz, the sensitivity can reach 152.0 pm/g , the working frequency band of the sensor is 5–300 Hz, the mass is 20 g, and the volume is about 22 cm^3 . Qiu et al. [17] proposed a symmetrical cantilever beam miniaturized low-frequency FBG acceleration sensor with a natural frequency of about 72 Hz, a sensitivity of about 681.7 pm/g in the operating range of 8–52 Hz, a mass of 0.7 g, and a volume of about 6.48 cm^3 . Although the sensor has a small volume, its low-frequency performance is not excellent enough. The studies above have promoted the development of cantilever-type FBG acceleration sensors to a certain extent; however, there is still a situation where the sensor volume is excessively increased in order to obtain better low-frequency characteristics, and the problem of considering the miniaturization of the sensor and the difficulty in effectively picking up low-frequency vibration signals urgently needs to be solved.

To solve the problem that FBG acceleration sensors based on cantilever beams are difficult to effectively pickup low-frequency vibration signals and that the sensors are large in size, a miniaturized low-frequency FBG acceleration sensor based on double cantilever beams is proposed. The FBG is pasted by the two-point attachment method; one end of the FBG is attached to the mass block, and the other end

is attached to the upper surface of the sensor by applying a certain pre-stress. Through theoretical derivation and analysis and optimization of cantilever dimension parameters by using the SolidWorks modeling software and the ANSYS finite element simulation software, the size of the sensor is reduced; the real sensor is developed, and a low-frequency vibration test system is established to test its main performance.

Structure design and theoretical analysis of the sensor

The pickup structure is a key component for measuring vibration. It principally relies on the relative displacement generated by the deformation of elastomer in vibration to yield the acceleration signal of external vibration. As shown in Fig. 1, the FBG acceleration sensor consists of an FBG, two mass blocks, double cantilever beams, and a stainless-steel housing. The two mass blocks are symmetrically placed on the upper and lower surfaces of the cantilever beam to constitute the spring-mass inertial vibration system of the acceleration sensor; the four wings of the cantilever beam are embedded in the sensor center, while the FBG is symmetrically attached to the surface of the mass block, and the housing by the two-point attachment method and a certain pre-stress is applied, thereby avoiding the chirping effects that may be caused by non-uniform strains in the grating region.

As shown in Fig. 1, the cantilever beams on both sides are strictly symmetrical, clamping the mass block to the sensor center to improve its axial sensitivity. When the test object vibrates, the sensor is subjected to inertia, and the mass block at the free end of the sensor vibrates vertically up and

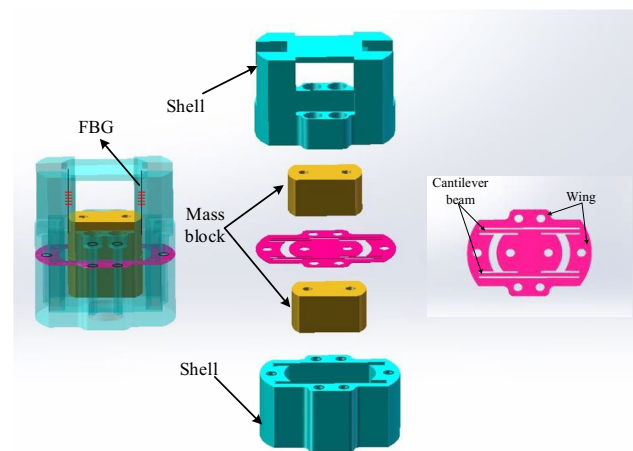


Fig. 1 Sensor structure diagram

down, thereby converting the displacement amplitude of the vibration into the strain value in the axial direction of FBG; the central wavelength of the reflection spectrum in FBG will change accordingly. By detecting the drift of the central wavelength, the magnitude of acceleration can be obtained, thereby achieving the measurement of external vibration.

The structural equivalent model of the sensor is shown in Fig. 2, where L is the length of the cantilever beam; M is the weight of the sensor's mass block; H represents the thickness of cantilever beam; y denotes the micro-displacement caused by the vibration; B stands for the width of the cantilever beam.

The sensor can be equivalent to a second-order single-DOF forced vibration model composed of a cantilever beam and a mass block, where the equivalent elastic stiffness K of the cantilever principally depends on the material and structural size of the cantilever beam and plays an important role in determining the sensitivity and natural frequency of the sensor [18]. In the coordinate system shown in Fig. 2a, the motion equation of the mass block is as follows:

$$My'' + \gamma y' + Ky + Ma = 0 \quad (1)$$

where γ denotes the damping constant of vibration system; K is the equivalent elasticity coefficient of the vibration system; a stands for the acceleration of the vibration signal to which the sensor is subjected.

When the forced vibration of the mass block causes the cantilever beam to deform, the strain ε in the cantilever beam is as follows:

$$\varepsilon = \frac{3FL}{2EBH^2} \quad (2)$$

where F is the inertial force on the mass block, and E represents the elastic modulus of the cantilever beam material.

The stretching or compression of FBG changes the period of the refractive index of fiber core, thus causing the reflection peak to shift and the central wavelength to change accordingly [19]. Since the cantilever and FBG are in the same plane, the deformation produced by the cantilever beam can be approximately regarded as the deformation of the FBG; hence, the following is true:

$$\Delta\lambda = \lambda(1 - P_e) \frac{3FL}{2EBH^2} \quad (3)$$

To better obtain low-frequency vibration signals, the sensor needs to have good sensitivity in a certain frequency band. The sensitivity S of the acceleration sensor can be obtained by combining Eqs. (3), $F = ma$, and $S = \Delta\lambda/a$ as follows:

$$S = \lambda(1 - P_e) \frac{3ML}{2EBH^2} \quad (4)$$

As shown in Eqs. (4), the sensor sensitivity S is related to the strain generated when the sensing element of the sensor is forced to vibrate. The sensitivity referred to in this paper is a peak-to-peak value, that is, $2S$.

The natural frequency of the FBG acceleration sensor determines the input signal frequency that can be measured; the natural frequency of the sensor is as follows:

$$F_0 = \frac{\omega_0}{2\pi} = \sqrt{\frac{2EBH^3}{3ML^3}} / 2\pi \quad (5)$$

As can be seen from Eqs. (4) and (5), thickness H , length L and width B of the cantilever beam are key parameters affecting the sensitivity and natural frequency of the sensor. Therefore, it is necessary to optimize the design of

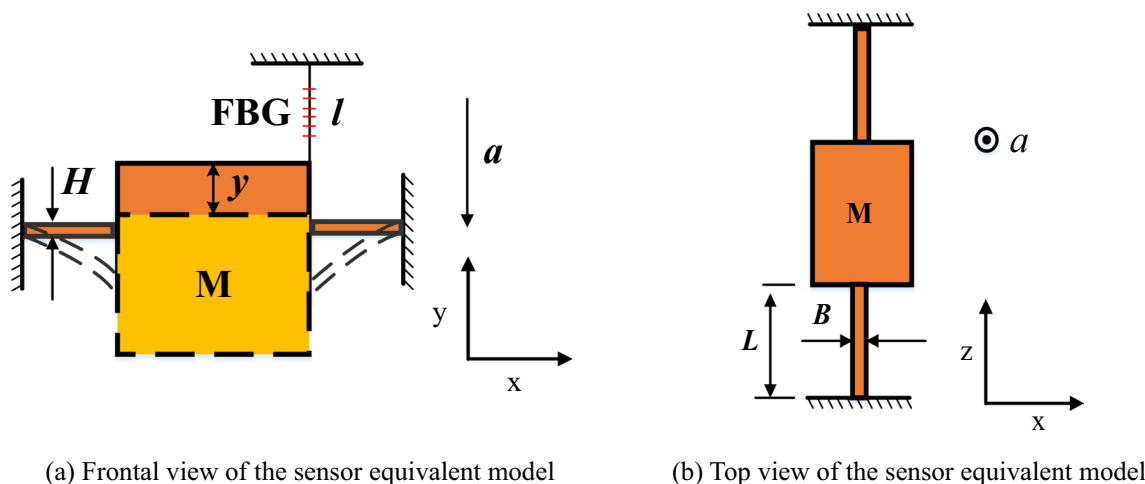


Fig. 2 Structural equivalence model of the sensor

the cantilever structural parameters to balance the natural frequency, sensitivity and sensor volume.

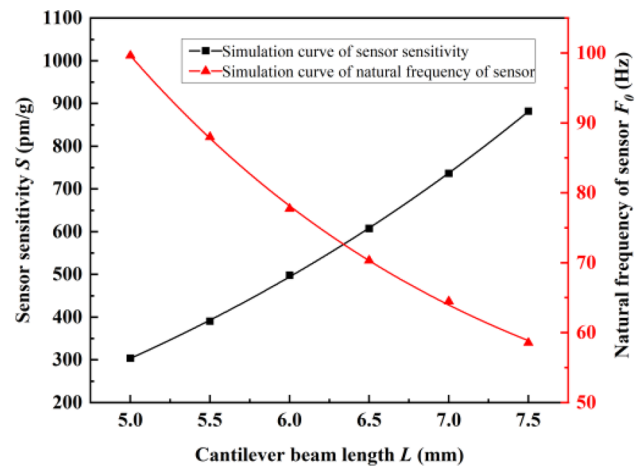
Simulation analysis

Structural parameter analysis

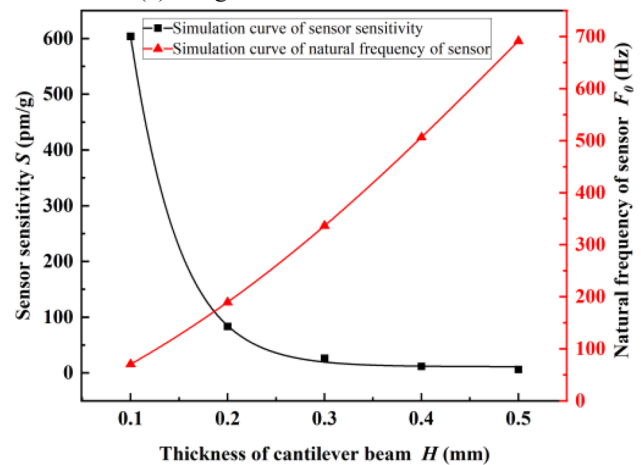
Natural frequency and sensitivity are two important performance indicators to evaluate FBG acceleration sensors. However, inevitable issues such as higher natural frequencies, lower sensitivity, and lower natural frequencies often result in larger mass limit the development of miniaturized low-frequency FBG acceleration sensors. Therefore, the cantilever structure needs to be optimized to ensure high low-frequency response characteristics under the condition of small volume. As can be seen from Eqs. (4) and (5), thickness H , length L and width B of the cantilever beam significantly affect the sensitivity and natural frequency of the sensor. Therefore, with other parameters defined, the SolidWorks software is used to model different sizes of cantilever beams, and the ANSYS Workbench is used to simulate the effects of these three key parameters on sensor sensitivity and natural frequency, as shown in Fig. 3.

The size of the sensing element of the sensor is changed by reducing the size of each cantilever beam and increasing the number of cantilever beams. Figure 3a discusses the effect of cantilever length L on sensor sensitivity S and natural frequency F_0 as it varies within 4.5–7.5 mm. As shown in Fig. 3a, the sensor sensitivity is positively correlated with the length of cantilever beam, while the natural frequency is negatively correlated with the length of the cantilever beam. In view of the engineering application requirements on low-frequency vibration monitoring and the goal of sensor miniaturization, the natural frequency of the sensor selected should be greater than 60 Hz, while the sensitivity should not be excessively low; hence, the length of the cantilever beam L can be greater than 6 mm and smaller than 7 mm.

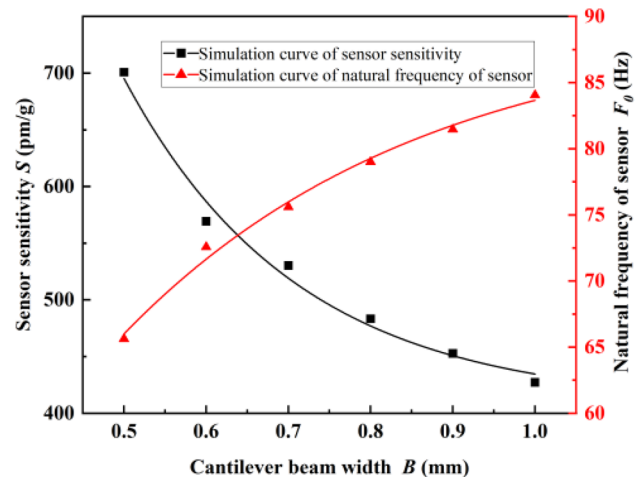
Figure 3b illustrates the effect of cantilever beam thickness H on sensitivity S and natural frequency F_0 of the sensor. When the cantilever beam thickness H changes between 0.1 and 0.6 mm, the sensor sensitivity S decreases with the increase in cantilever beam thickness H , while natural frequency F_0 increases with the increase in cantilever beam thickness H . when $0.1 \text{ mm} \leq H \leq 0.2 \text{ mm}$, the sensitivity S curve exhibits an obvious downward trend; when $0.2 \text{ mm} < H < 0.6 \text{ mm}$, the downward trend levels off. To meet the sensor’s requirements for sensitivity and natural frequency, it is desirable that $H = 0.2 \text{ mm}$.



(a) Length L of the cantilever beam



(b) Thickness H of the cantilever beam



(c) Width B of the cantilever beam width

Fig. 3 Effects of structural parameters on sensor performance indicator S and F_0

Figure 3c illustrates the effect of cantilever beam width B on sensitivity and natural frequency F_0 of the sensor. When the cantilever beam width B changes between 0.4 and 1.1 mm, the sensor sensitivity S decreases with the increase in cantilever beam width B , while natural frequency F_0 increases with the increase in cantilever beam width B . To achieve high sensitivities, width B of the cantilever beam should be as small as possible; considering the material selection of the cantilever beam and the limitations of the actual processing conditions, it is desirable that $B=0.5$ mm.

In reference to the design objectives and the engineer application requirements, as well as material selection and processing conditions, the structural parameters of the sensor developed are shown in Table 1.

ANSYS simulation software

To further study the dynamic response characteristics of the miniaturized low-frequency FBG acceleration sensor with double cantilever beams, the sensor is modeled by the SolidWorks software, and the model is imported into ANSYS software for static stress analysis and modal simulation analysis of the sensor structure, so as to demonstrate the data results obtained by the theoretical analysis and provide assistance for sensor processing. 65Mn spring steel with high elasticity is chosen as the cantilever beam material (the Young's modulus $E=201$ Gpa; the Poisson's ratio $\mu = 0.28$); H62 brass with high density is chosen as the mass block material (the elasticity modulus is 100 Gpa, and the density is 8500 kg/m³).

To ensure that the sensitive structure of the sensor can function properly during forced motion, it is necessary to perform static stress analysis on the sensor. Firstly, a fixed constraint is applied to the bottom of the sensor model, and the connection between the components is set as a fully bound support constraint; since the low-frequency vibration table can provide an acceleration of 0.5 g maximum,

Table 1 Structural parameters of sensor

Structure parameters	Numerical values
The mass of the mass block M	1.4 g
Cantilever beam length L	6.5 mm
Cantilever beam width B	0.5 mm
Cantilever beam thickness H	0.2 mm
Young's modulus E of optical fiber	72.9×10^9 Pa
Effective length l of optical fiber	5 mm
Outer diameter D of optical fiber	0.125 mm
FBG central wavelength λ_B	1550.2 nm
Cross-sectional area A_f of optical fiber	1.23×10^{-8} m ²
Effective elasto-optical coefficient of optical fiber P_ϵ	0.22

an acceleration of 1 g in the Y axis can be applied to the whole model during simulation. As shown in Fig. 4a, when the sensor is forced to move, the stress is principally distributed on the cantilever beam, and the maximum stress value is 87.45 Mpa. After the 65Mn spring steel is quenched, the yield strength of the material is generally not less than 800 Mpa, which fully meets the requirements and can guarantee the proper operation of the cantilever beam structure. When constraints are applied and the acceleration is constant, the displacement cloud chart of the sensor in the Y axis direction is shown in Fig. 4b; it can be concluded that the deformation at the free end of the sensor is the greatest; the deformation gradually decreases from the free end to the support end, and the maximum displacement at the free end is 51 μ m. Then, an acceleration of 1 g in the X and Z axes is applied to the sensor as a whole to yield the transverse equivalent displacement diagram of the model. As shown in Fig. 4c and d, the maximum displacement of the free end is 1.8 μ m and 0.45 μ m, respectively.

According to the results of the static stress analysis of the sensor, the modal analysis of the sensor model is performed. In modal analysis, the model is meshed and the first-two-order modal frequencies of the model are simulated and analyzed, as shown in Fig. 5. As shown in Fig. 5, the first-order and second-order modal frequencies of this model are 69.82 Hz and 82.36 Hz, respectively, and its natural frequency is 69.82 Hz. There is little difference between the first-order and second-order modal frequencies, indicating that the structure has weak resistance to cross-interference, and other axial vibration excitations may cause cross-interference to the sensor.

Experiment system setup and testing process

Experiment system setup

The fiber Bragg grating used in the sensor is a single-mode fiber with a central wavelength of 1550.2 nm, a reflectivity of $\geq 90\%$, a grating length of 5 mm and a full width at half maximum of 0.4 nm. The reflection spectrum is shown in Fig. 6.

To test whether the developed sensor can meet the research expectations, a low-frequency vibration testing system consisting of a low-frequency vibration system and a fiber-optic sensing system is established, as shown in Fig. 7. The low-frequency vibration system adopts the low-frequency vibration table of the Institute of Geophysics, China Earthquake Administration; during the experiment, the sensor is fixed on the top of the vibration table, and a high-precision fiber-optic interrogator is connected to display the wavelength change of the optical fiber in real time on the PC side; the low-frequency vibration test is performed

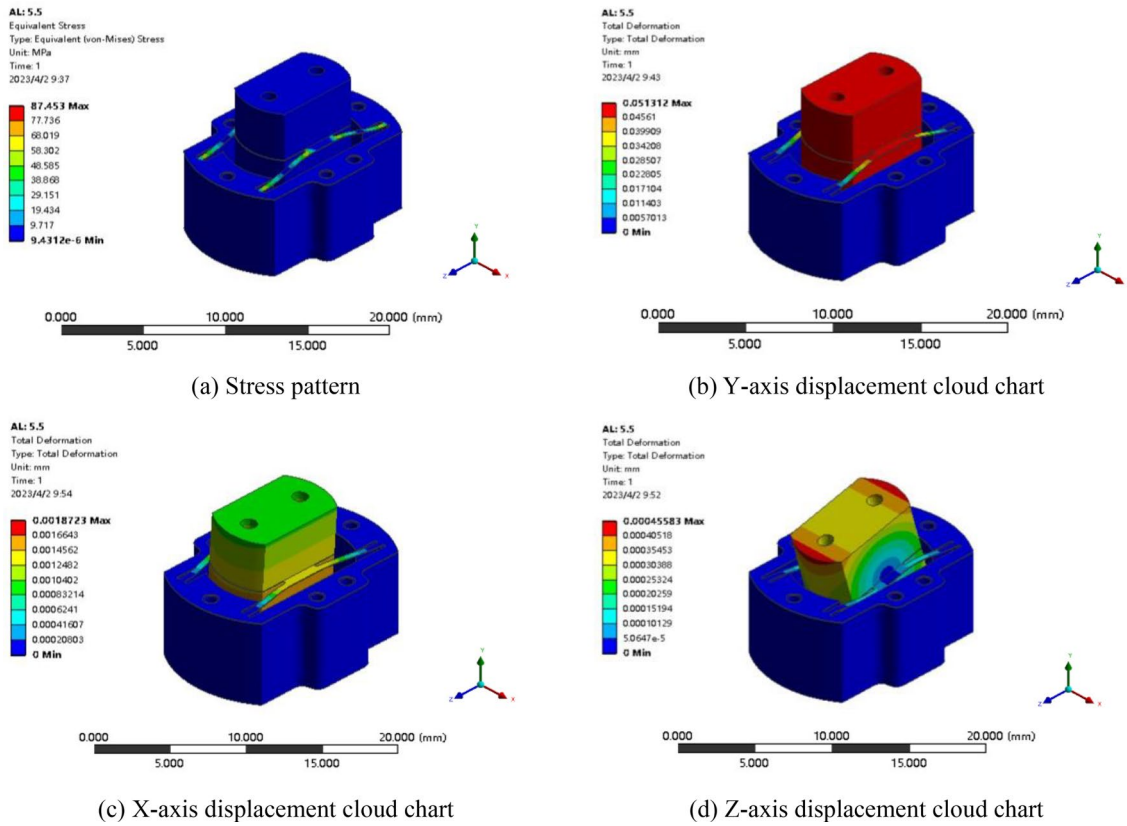


Fig. 4 Static stress analysis of the structure

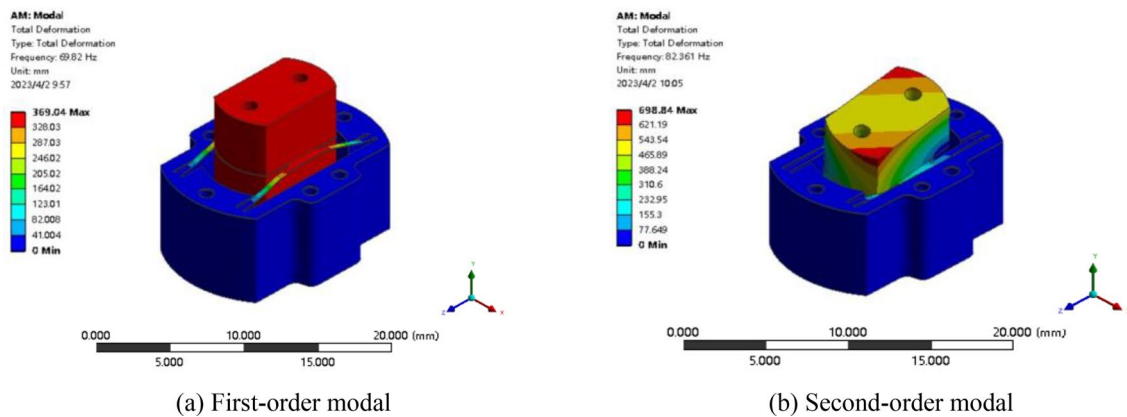


Fig. 5 Modal analysis of the structure

with a sampling rate of 1 kHz, as shown in Fig. 7a. The technical indicators of the low-frequency vibration table are as follows: The frequency range is 0.01–160 Hz; the maximum displacement is 0.15 m(p-p); the maximum speed (peak) is 0.1 m/s; the maximum acceleration (peak) at full load is 5 m/s²; the maximum load is 18 kg; the displacement distortion

is ≤ 1%; the lateral vibration ratio of acceleration is ≤ 3%. The fiber-optic sensing system comprises the FBG interrogator MWY-FBG-CS800 of Beijing Weiyun Technology Co., Ltd., and the interrogator displays the waveform and value of the wavelength change of FBG on the PC side, as shown in Fig. 7b.

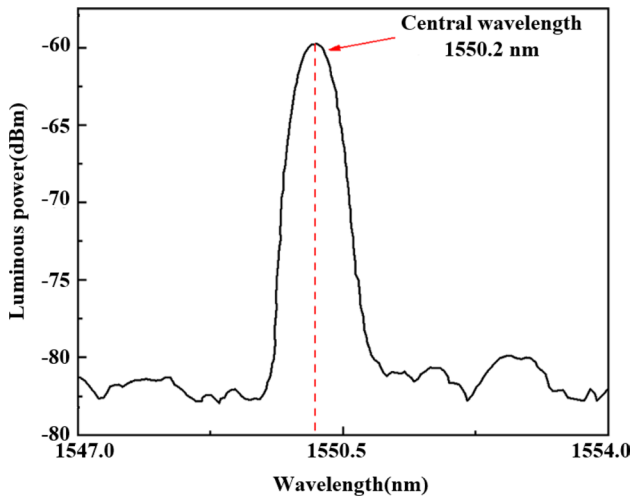


Fig. 6 Reflection spectrum of FBG

Experiment testing process

The sensor is fixed on the table surface; the vibration frequency of the vibration table is set up, and the actual acceleration value of the vibration table is acquired in real time by the laser absolute method. Due to the maximum amplitude limitation of the low-frequency vibration table, the smaller the frequency value of the vibration signal generated by the vibration table, the smaller the acceleration value that can be provided. An acceleration value of 2.0 m/s² can be selected in the frequency range of 2–100 Hz, while in the frequency range of 0.01–2 Hz, the vibration table cannot provide an acceleration of 2.0 m/s². The specific vibration parameters are shown in Table 2.

Sensor performance test

Output response test

The performance test based on the low-frequency vibration parameters provided in Table 2 yields the overall output response of the sensor, as shown in Fig. 8.

As shown in Fig. 8, when the acceleration is 2 m/s² and the vibration reaches the natural frequency, the wavelength change of FBG is the largest. At this point, the excitation frequency of the vibration table is close to the resonant frequency of the sensor, and the amplitude of the vibration response will increase sharply, thereby resulting in resonance. When the vibration frequency is less than 1 Hz, the frequency values of the five signal segments are 0.1 Hz, 0.2 Hz, 0.3 Hz, 0.5 Hz, and 0.6 Hz, respectively. The signals present favorable sinusoidal waveforms, indicating that the sensor can achieve vibration signal measurement in the frequency range of 0.1–1 Hz.

When the output response characteristics of the sensor are tested, the following 6 data points are selected with reference to (acceleration a, frequency f) for analysis: (0.02 m/s², 0.1 Hz), (0.10 m/s², 0.2 Hz), (1.00 m/s², 1 Hz), (1.96 m/s², 10 Hz), (2.00 m/s², 30 Hz), and (2.12 m/s², 50 Hz). The time series signals are subjected to the Fast Fourier Transform (FFT) by the Periodogram Method based on the Parseval’s theorem to yield the frequency domain response, which verifies the frequency value of the time domain signal and identifies the noise distribution; the measured time domain signal and frequency domain response from the FBG acceleration sensor are shown in Fig. 9.

FBG acceleration sensors are generally in the low-frequency range, and when the acceleration value of the



Fig. 7 Low-frequency vibration test system

Table 2 Vibration parameters of the low-frequency vibration test system

Frequency (Hz)	0.01	0.05	0.1	0.2	0.3	0.5	0.6	1	2	5
Acceleration (m/s ²)	0.0001	0.0050	0.0204	0.1083	0.2063	0.5342	0.5157	1.019	1.975	1.985
Frequency (Hz)	10	20	30	40	50	60	70	80	90	100
Acceleration (m/s ²)	1.964	1.993	2.001	1.999	2.116	1.965	1.998	1.999	1.996	1.995

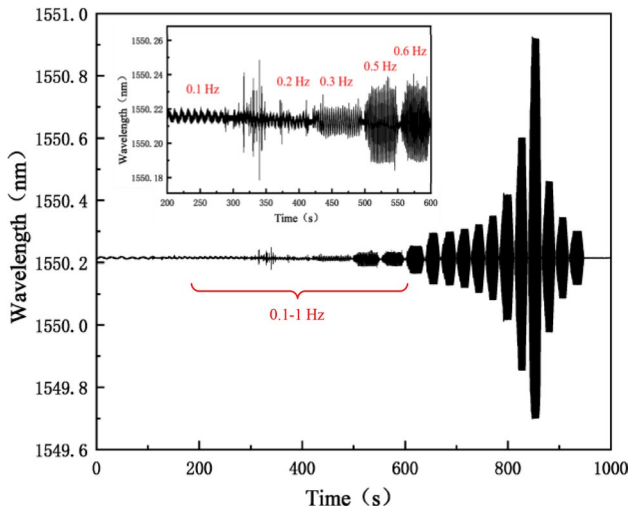


Fig. 8 Total waveform diagram

excitation signal is small, their ability to pickup signals is weak, the signal-to-noise ratio is low, and the signal output waveform may have burrs. As shown in Fig. 9a–c, under the excitation of low-frequency and low-acceleration vibration signals, the sensors can better pickup the sinusoidal excitations of external inputs and can clearly display the

picking up of vibration signals. As shown in Fig. 9d–f, when the frequency value of the excitation signal is large and the acceleration value is 2 m/s^2 , the vibration signal value picked up by the sensor presents an excellent waveform, indicating that the stress of FBG is uniform and there are not chirps and multipeaks. In the frequency domain response diagrams (Fig. 9g–l) obtained through the Fast Fourier Transform (FFT), the abscissa value of the highest point of the graph is the frequency value of the corresponding time domain signal, and the resulting test frequency is consistent with the time domain signal frequency; in addition, the noise power at other frequencies is low, and the signal-to-noise ratio of the sensor is high. From the above analysis, it can be seen that the sensor has favorable vibration signal pick-up capability in the low-frequency band.

Amplitude-frequency response test

The amplitude-frequency response characteristics of the sensor are tested, and the sensor is secured on the vibration table. The sinusoidal excitation signals with an acceleration amplitude of $0.2 \text{ g} (g = 10 \text{ m/s}^2)$ are set up based on the vibration frequencies set forth in Table 2, and a sweep test is performed on the sensor. When the approximate range of the sensor’s natural frequency is identified, the test is repeated

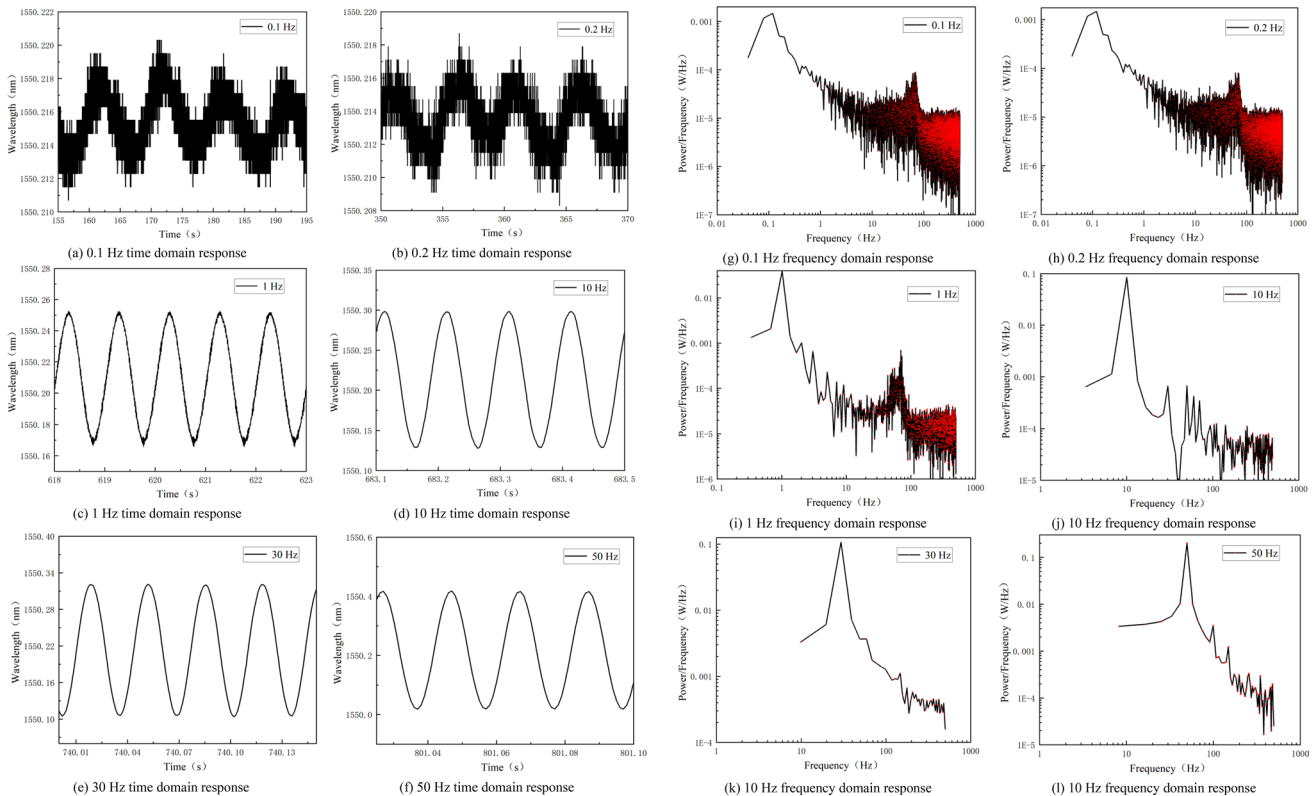


Fig. 9 Sensor output response curve

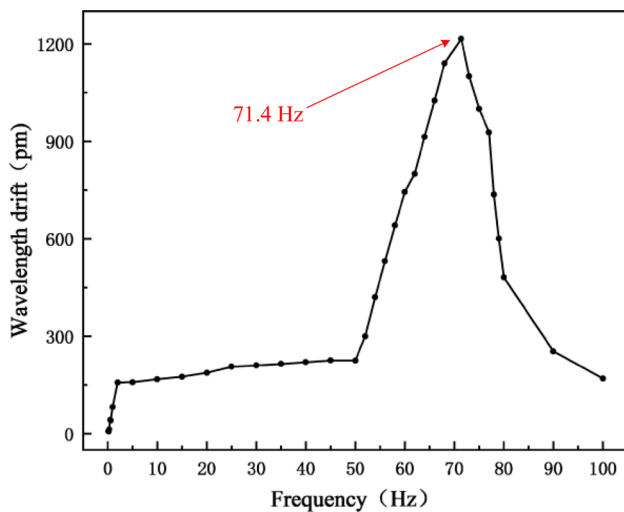


Fig. 10 Amplitude-frequency response of the FBG accelerometer

in steps of 2 Hz. Meanwhile, the wavelength changes of the FBG sensors collected by the FBG interrogator are recorded; the amplitude-frequency characteristic curve of the sensor is yielded by experimental data processing, as shown in Fig. 10.

As shown in Fig. 10, the natural frequency of the sensor is about 71.4 Hz, and the response is relatively gentle within the frequency range of 2–50 Hz; the experimental measurement of the natural frequency is similar to the simulation calculation, and the slight error may result from the cured UV adhesive-induced creep.

To verify the results of the amplitude-frequency response experiment, an impact response test is performed. Compared with the excitation signal, the impact signal is an unsteady transient signal and contains abundant vibration information, which can fully reflect the response characteristics of the acceleration sensor. The method of instantaneous tapping on the vibration table is used in the experiment to simulate the generation of an impact signal, and the impact response test results are shown in Fig. 11.

As shown in Fig. 11, the FBG acceleration sensor can effectively reflect the impact excitation; by subjecting the time domain data to FFT, the frequency domain response diagram of the sensor can be achieved. It can be concluded that the natural frequency of the sensor is about 72 Hz, which is consistent with the simulation results and the experimental results of the sensor amplitude-frequency response.

Linear response test

To identify the sensitivity characteristics of the sensor under different frequency excitations, when the vibration frequency

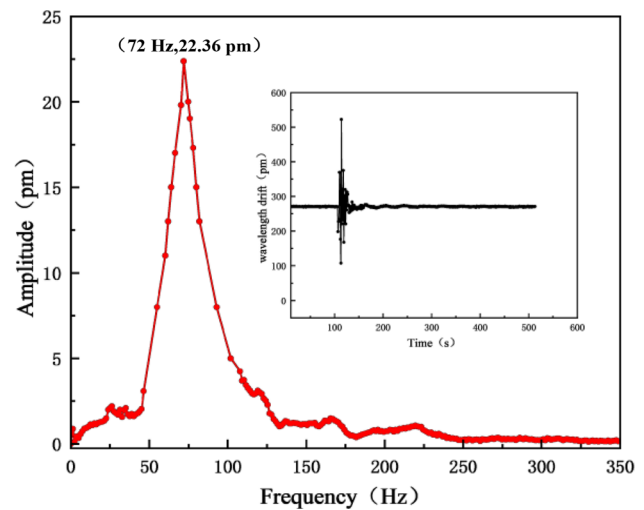


Fig. 11 Impact response curve of the sensor

is 10 Hz and 30 Hz, respectively, the acceleration amplitude is adjusted so that the acceleration amplitude of the excitation signal increase from 0.05 to 0.5 g in steps of 0.05 g. Record the wavelength drift of the sensor, repeat each experiment three times and take the average value to obtain the curve of wavelength drift with acceleration at different frequencies, as shown in Fig. 12.

As shown in Fig. 12, when the frequency of the excitation signal is 10 Hz and 30 Hz, respectively, the sensitivity of the acceleration sensor is 980.3 pm/g and 1065.2 pm/g, respectively; the linearity is 99.98% and 99.96%, respectively; deviations occur at certain points, which may be related to the stability of the demodulation system and the interference from external signals.

In addition to sensitivity, dynamic range is also one of the important parameter indicators of the sensor. The dynamic range D_R is related to the maximum wavelength drift λ_{\max} and the minimum wavelength drift λ_{\min} , and the relational expression is as follows:

$$D_R = 20 \lg \left(\frac{\lambda_{\max}}{\lambda_{\min}} \right) \quad (6)$$

The maximum wavelength drift λ_{\max} is principally restricted by the elastic deformation range of the elastic components of the sensor and the FBG pre-stress; the minimum wavelength drift λ_{\min} is principally dependent on the resolution of the FBG demodulation system. In the sensitivity test experiment of this sensor, the maximum wavelength drift output is 531 pm, and the FBG interrogator resolution used in the experiment is 0.1 pm; the dynamic range of the sensor is calculated to be up to 74.5 dB.

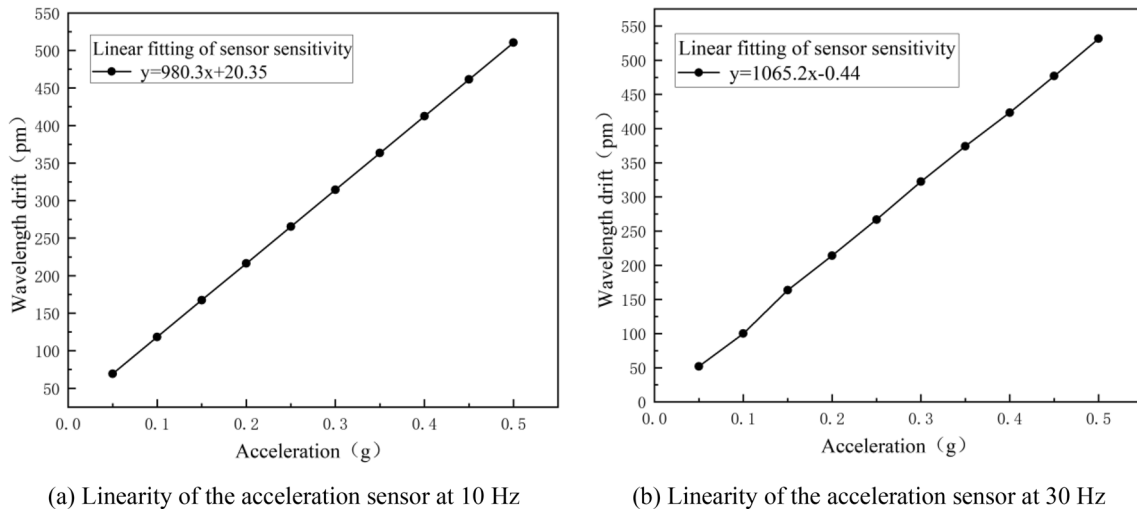


Fig. 12 Linear response of the FBG acceleration sensor

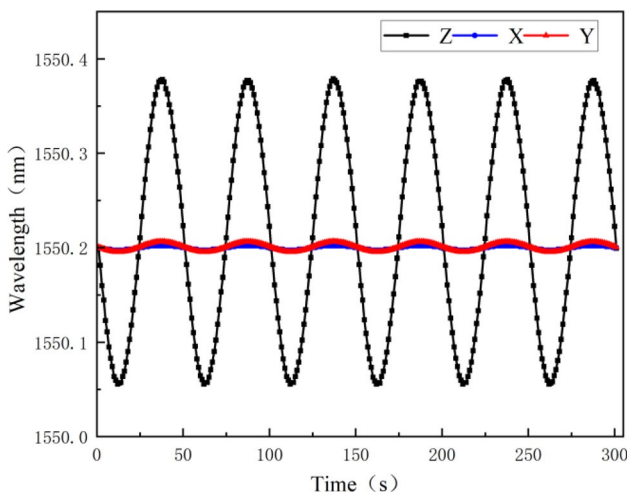


Fig. 13 Transverse interference immunity test of the sensor

The sensitivity and transverse immunity experiment

Transverse interference immunity characteristics are also an important performance criterion to consider for Single degree of freedom acceleration sensors. In the experimental test, the sensors are installed longitudinally along the sensor by rotating 90°, respectively, so that the main vibration direction of the sensor is perpendicular to the vibration direction of the vibration table; a transverse interference immunity test is performed as shown in Fig. 13.

As shown in Fig. 13, under the same excitation frequency and amplitude, the wavelength drift is about 330 pm in the Z axis, about 14 pm in the Y axis, and about 8 pm in the X axis. It indicates that the transverse interference of the sensor in the Y axis is not higher than 4.2%, while the transverse interference in the X axis is not higher than 2.4; hence, it

can be concluded that the sensor can effectively suppress the effects of transverse interference.

It is observed from Table 3 that the miniaturized low-frequency FBG acceleration sensor based on double cantilever beams proposed in this paper is smaller in size and higher in sensitivity; furthermore, it enables low-frequency vibration measurement in the range of 2–50 Hz, and the sensor behaviors are not deteriorated; hence, the sensor substantially meets the requirements on acquisition of low-frequency vibration signals in engineering. Compared with other FBG acceleration sensors, the structure employs the method of reducing the size of individual cantilever beams and increasing the number of cantilever beams to effectively pickup low-frequency vibration signals while minimizing the sensor volume.

Conclusion

Aiming at the problem that the cantilever-type FBG acceleration sensors are difficult to effectively pickup low-frequency vibration signals and that they are large in size, the paper proposes a double cantilever beams-based miniaturized low-frequency FBG acceleration sensor; by reducing the size of cantilever beam and increasing the number of cantilever beams, the volume of the sensing element is reduced, thereby reducing the volume of the sensor. The designed sensor is design-optimized and performance-tested by integrating simulation analysis with experimental verification. The research finding suggests that the natural frequency of the sensor is about 71.4 Hz; the low-frequency vibration signals can be effectively picked up in the frequency range of 0.1–2 Hz; favorable linearity is observed in the operating frequency band of 2–50 Hz; the sensitivity is

Table 3 Comparison of FBG acceleration sensors

Research Group	Mass block mass (g)	Sensor volume (cm ³)	Sensitivity (pm/g)	Measurable frequency range (Hz)
Liu et al. [10]	35	56	8.58	4–30
Lim et al. [11, 15]	5	70	7.1	20–100
Khan et al. [12]	23	25	46–306	20–40, 150–200
Parida et al. [13]	16	2	821	5–40
Jiang et al. [14]	41	52	59.3	1–60
Xiang et al. [15]	63	235	75	50–100
Liu et al. [16]	20	22	152	5–300
This work	1.4	7	1022.8	2–50

about 1022.8 pm/g, and the dynamic range is 74.5 dB; the transverse interference is not higher than 4.2%. In addition, temperature compensation has not been considered for the sensor, so the sensor may fail in operating environments with significant temperature differences. The temperature interference can be eliminated by introducing dual optical fibers in the future, so that the sensor can be applied to the research of engineering low-frequency vibration signal acquisition and seismic monitoring as soon as possible.

Acknowledgements This study was financially supported by the Science and Technology Innovation Program for Postgraduate students in IDP subsidized by Fundamental Research Funds for the Central Universities (Grant No. ZY20230323), the Fundamental Research Funds for the Central Universities (Grant No. ZY20215142), the 2020 Educational Research and Teaching Reform Project of the School of Disaster Prevention Science and Technology (Grant No. JY2020A12).

References

- X. Qin, Z. Zhen, Z.L. Xin, Influence of the rubber end plate on the hysteretic performance of SC-BRBs and structural seismic design. *Eng. Struct.* **242**, 112475 (2021)
- Y.S. Tang, J.G. Cang, Y.D. Yao, C. Chen, Displacement measurement of a concrete bridge under traffic loads with fibre-reinforced polymer-packaged optical fibre sensors. *Adv. Mech. Eng.* **12**(3), 10538 (2020)
- F.F. Liu, Y.T. Dai, J.M. Karanja, M.H. Yang, A low frequency FBG accelerometer with symmetrical bended spring plates. *Sensors*. **17**(1), 206–206 (2017)
- J.S. Dong, W.Y. Ying, Z.F. Xiang, S.Z. Hui, W. Chang, A high-sensitivity FBG accelerometer and application for flow monitoring in oil wells. *Opt. Fiber. Technol.* **74**, 103128 (2022)
- N. Gutiérrez, P. Galvín, F. Lasagni, Low weight additive manufacturing FBG accelerometer: design, characterization and testing. *Measurement* **117**, 295–303 (2018)
- T.L. Li, J.X. Guo, Y.G. Tan, Z.D. Zhou, Recent advances and tendency in fiber Bragg grating-based vibration sensor: a review. *IEEE. Sens. J.* **20**(20), 12074–12087 (2020)
- Y.T. Yi, J. Ke, L. Lei, T.Y. Lei, Z.Z. Yue, Dynamic response mechanism analysis of hinged FBG acceleration sensor. *Opt. Fiber. Technol.* **74**, 103131 (2022)
- W.X. Qiang, W. Xue, L.S. Li, H. Sheng, G. Qiang, Y.B. Li, Cantilever fiber-optic accelerometer based on modal interferometer. *IEEE. Photonic. Tech. L.* **27**(15), 1632–1635 (2015)
- H. Li, S. Rui, Q.Z. Chao, H.Z. Ming, L.Y. Nan, A multi-cantilever beam low-frequency FBG acceleration sensor. *Sci. Rep-uk.* **11**(1), 1–11 (2021)
- Q. Liu, Z.A. Jia, H. Fu, Double cantilever beams accelerometer using shortfiber Bragg grating for eliminating chirp. *IEEE. Sens. J.* **16**(11), 6611–6616 (2016)
- W. Udos, Y.S. Lee, K.S. Lim, Z.C. Ong, M.K.A. Zaini, H. Ahmad, Signal enhancement of FBG-based cantilever accelerometer by resonance suppression using magnetic damper. *Sensor. Actuat. A-phys.* **304**, 111895 (2020)
- M.M. Khan, N. Panwar, R. Dhawan, Modified cantilever beam shaped FBG based accelerometer with self temperature compensation. *Sensor. Actuat. A-phys.* **205**, 79–85 (2014)
- P.O. Prakash, N. Jagannath, A. Sundarajan, Design and validation of a novel high sensitivity self-temperature compensated fiber Bragg grating accelerometer. *IEEE. Sens. J.* **19**(15), 6197–6204 (2019)
- S.D. Jiang, Y.Y. Wang, F.X. Zhang, Z.H. Sun, C. Wang, A high-sensitivity FBG accelerometer and application for flow monitoring in oil wells. *Opt. Fiber. Technol.* **74**, 103128 (2022)
- L.H. Xiang, Q. Jiang, Y.B. Li, R. Song, Design and experimental research on cantilever accelerometer based on fiber Bragg grating. *Opt. Eng.* **55**(6), 1–6 (2016)
- Q.P. Liu, X. He, X.G. Qiao, T. Sun, K.T.V. Grattan, Design and modeling of a high sensitivity fiber Bragg grating-based accelerometer. *IEEE. Sens. J.* **19**(14), 5439–5445 (2019)
- Z.C. Qiu, K. Su, J.Q. Zhang, R. Sun, Y.T. Teng, A miniaturized low-frequency FBG accelerometer based on symmetrical cantilever beam. *IEEE. Sens. J.* **23**(6), 5831–5840 (2023)
- S. Saha, K. Biswas, A comparative study of fiber Bragg grating based tilt sensors. *Review. Com. Eng. Stud.* **4**(1), 41–46 (2017)
- L.T. Li, D.S. Zhang, H. Liu, Y.X. Guo, F.D. Zhu, Design of an enhanced sensitivity FBG strain sensor and application in highway bridge engineering. *Photonic. Sens.* **4**(2), 162–167 (2014)

Publisher's Note Springer Nature remains neutral with regard to jurisdictional claims in published maps and institutional affiliations.

Springer Nature or its licensor (e.g. a society or other partner) holds exclusive rights to this article under a publishing agreement with the author(s) or other rightsholder(s); author self-archiving of the accepted manuscript version of this article is solely governed by the terms of such publishing agreement and applicable law.